Effective Removal of Cationic Dyes from Aqueous Solutions by Using Black Cumin (*Nigella sativa*) Seed Pulp and Biochar

Sedef Sismanoglu,[a] Mehmet Kuddusi Akalin,[b,*] Gulen Oytun Akalin,[c] and Fatıma Topak [b]

Black cumin seed pulp (C), as well as biochar (CC) produced *via* pyrolysis of black cumin seed pulp were used to remove methylene violet 2B (MV) and basic yellow 28 (BY28) from aqueous solution. Adsorption isotherms and kinetics were applied at 10, 25, and 35 °C. The adsorption of methylene violet 2B and basic yellow 28 on the black cumin seed pulp and biochar surface was exothermic; the heat of adsorption values were lower than 0. The adsorption capacities of BY28-C, BY28-CC, MV-C, and MV-CC were 212.8, 625, 164, and 909 mg g^{-1} at 25 °C, respectively. The adsorption of black cumin seed pulp and biochar data were examined with the Freundlich, Langmuir, Temkin, Dubinin-Radushkevich (D-R), and Flory-Huggins (F-H) isotherm models. The kinetics of the adsorption were fitted to the pseudo first-order and pseudo second order equations. The pseudo second order equation gave a better fit than the pseudo first-order equation.

DOI: 10.15376/biores.18.2.3414-3439

Keywords: Black cumin seed pulp; Biochar, BY28; MV; Adsorption

Contact information: a: Department of Chemistry, Karabuk University, 78050, Karabuk, Turkey; b: Department of Environmental Engineering, Karabuk University, 78050, Karabuk, Turkey; c: Medical Laboratory Program, Department of Medical Services and Techniques, Vocational School of Health Service, Aksaray University, 68100, Aksaray, Turkey;
** Corresponding author: mehmetakalin@karabuk.edu.tr*

INTRODUCTION

Synthetic dyes are potential water pollutants that are widely used by the textile industry; they cause problems because of their toxicity and their coloring (Han *et al.* 2015; Singh *et al.* 2022). Adsorption is an effective way to remove dyes from wastewaters, and activated carbon is widely used for this purpose. However, the activation process increases the cost and energy consumption of the process. Chemical activation is widely used to produce activated carbon from biomass. However, using chemicals for the activation increases the cost of the process and causes hazardous effects to the environment (Choi *et al.* 2019; Vigneshwaran *et al.* 2021). Therefore, using an adsorbent that is abundant in nature, or a waste or a by-product of a process becomes important. Biochar is carbon-rich material that is obtained *via* thermochemical conversion of biomass. Despite having low adsorption capacities, biochar is a potential alternative to activated carbon in water treatment due to its low cost and not using chemicals for the activation (Zazycki *et al.* 2018; Choi *et al.* 2019). Agricultural byproducts that have low economic value and biochar produced from those materials are good alternative adsorbents for the removal of dyes from wastewater.

Black cumin is used in the treatment of cancer, diabetes, asthma, and kidney diseases due to the different active pharmaceutical components in its content. It is grown in Southwest Asia and Eastern Mediterranean countries (Zent 2019; Yimer *et al.* 2019; Can 2020). In Turkey, black cumin is grown in provinces such as Mersin, Gaziantep, Isparta, Burdur, Uşak, and Bursa (Koşar and Özel 2018; Can 2020). While black cumin seed production in Turkey was 161 tons in 2012 (2299 decares), it increased to 3603 tons in 2019 (37085 decares). When considering the foreign trade data of black cumin, it can be seen that 2647.5 tons of black cumin seed ($2.53 million) was imported in the same year, equal to the export of 592.4 tons ($1.23 million) of black seed in 2019 (Can 2020). Black cumin is used as a health supplement and condiment, as well as spice in the food industry, and the pulp is used as a filler in the production of environmentally friendly polymer composites (Yimer *et al.* 2019; Sismanoglu *et al.* 2022). It is used as feed in animal nutrition in order to prevent environmental pollution and create added value from the pulp part that is released during the production of black seed oil (Zent 2019).

A natural agricultural product, *Lolium perenne* seed, was used for the removal of safranine T, and the adsorption capacity q_{max} was 323 mg/g at 25 °C and pH 7 according to the Langmuir isotherm model (Karadeniz *et al.* 2023). In another study, *Cotinus coggygria* leaves were used as an adsorbent for the removal of safranine T. The maximum adsorption capacity was 2000 mg/g at 55 °C and pH=7 (Ugraskan *et al.* 2022). Temiz and co-workers produced microbeads composites with the combination of *Capsella bursa-pastoris* and chitosan for the removal of methylene blue, and the maximum adsorption capacity was reported as 222 mg/g at 25 °C. (Temiz *et al.* 2022). *Valeriana officinalis* roots were used as an adsorbent for the adsorption of anionic Congo red and cationic crystal violet dyes. At 25 °C, the Langmuir q_{max} values were 166.7 and 476.2 mg/g for Congo red and Crystal violet, respectively (Akdemir *et al.* 2022). In another study, *Rumex acetosella* was used as an adsorbent for adsorption of crystal violet, and the maximum adsorption capacity was reported as 434.8 mg/g at 25 °C and pH=7 to 8 (Erdogan *et al.* 2022). Judas tree (*Cercis siliquastrum*) seeds were used as an adsorbent in the adsorption of Basic blue 9 and Basic green 4 dyes. The q_{max} values for the Langmuir isotherm were reported as 500 and 244 mg/g at 25 °C for BB and BG, respectively (Isik *et al.* 2022).

Compared with other studies with basic yellow 28 (BY28), the adsorbent (GAC-HB) was added to 200 mL of basic yellow 28 dye solution on coconut shell charcoal granular activated carbon. Different studies were conducted on sorbent dose, initial dye concentration, solution pH 9, GAC-HB dose 0.8 g/L, and contact for 2 h. The optimum conditions for BY28 were determined. The Langmuir q_{max} value was 769 mg/g (Dao *et al.* 2013). Activated carbon produced from *Persea americana* nut (PAN) was used with V= 50 mL BY 28 (100 mg/L) in at ambient temperature and Langmuir maximum uptake (q_{max}) at 0.2 g/L dosage was 325 mg/g (Regti *et al.* 2017). The adsorbent is related to the adsorption of BY28 to low-cost natural red clay (NRC). For adsorption studies, contact time, initial concentration, pH, adsorbent mass, and temperature were studied as 1 to 180 min, 50 to 300 mg/L, 3-10, 0.5 to 10 g/L, and 25 to 40 °C, respectively. Langmuir maximum monolayer adsorption capacity q_{max} was 370 mg/g. The adsorption of basic yellow 28 dye on adsorbent Ca-bentonite was investigated at pH 7.0 for temperatures of 20 and 40 °C. The Langmuir maximum monolayer adsorption capacity (q_{max}) of Ca-bentonite was determined as 94.3 mg/g at 20 °C and 99.0 mg/g at 40 °C (Kalpaklı *et al.* 2014).

In another study, adsorption of methyl violet (MV) onto biochars from crop residues showed the following results: peanut straw charcoal > soybean charcoal > rice husk charcoal. They were rinsed with 0.200 g biochar in a water bath at a constant temperature of 25 ± 1 °C for 2 h and after 22 h it was adjusted at pH 8 to 10 and centrifuged. The Langmuir maximum uptake (q_{max}) was 256, 178, and 123 mg/g, respectively for peanut charcoal > soybean charcoal > rice husk charcoal (Xu *et al.* 2011). Adsorbent *Casuarina equisetifolia* needle (CEN) was used to extract methyl violet 2B (MV) from aqueous solutions. Optimal conditions were at room temperature with a contact time of 2 h and no pH adjustment was required. From the experimental data, the maximum adsorption capacity was found as 165 mg/g for the Langmuir model (Dahri *et al.* 2013). Modified *Ceiba pentandra* sawdust has been investigated as an adsorbent for the removal of methyl violet dye from aqueous solutions. The effective pH for methyl violet adsorption was 7. Equilibrium was reached in 30 min. The Langmuir maximum capacity (q_{max}) was 16 mg/g (Astuti and Fatin 2018). Pine bark was activated with HNO_3 as an adsorbent and used as activated carbon (AC) to remove textile dye (methyl violet MV) from aqueous solutions. The variables were the pH of the solution (3 to 11), activated carbon (from pine bark) amount (0.01 to 0.13 gm), MV dye concentration (5 to 50 mgL^{-1}), and solution temperature (10 to 50 °C). The maximum adsorption capacity of the dye MV at AC was 95.13 mg/g (Bader *et al.* 2019). The adsorption of methyl violet and malachite green 2B by phthalate-functional sugarcane pulp (SPA) was investigated. SPA (5, 10, 15, 20, 25, 30, 35) mg was added to 20 mL of 25 mg L^{-1} methyl violet 2B solution, shaken again at 180 rpm for 180 min. The q_{max} of MV 2B was 60.5 mg g^{-1} (Ariani *et al.* 2018).

In this study, black cumin seed pulp, which has a low economical value, and biochar, which was produced via pyrolysis of black cumin seed pulp, were used as low-cost adsorbents for the removal of methyl violet 2B and basic yellow 28. The characterization of the adsorbent was performed before and after adsorption by FTIR/ATR, TGA, and SEM. The removal of methylene violet 2B (MV) and basic yellow 28 (BY28) were tested, and different kinetic and adsorption isotherms models were applied.

EXPERIMENTAL

Feedstock and Chemicals

Black cumin (*Nigella sativa*) seed pulp was obtained at no cost from Bağdat Spices Co., Ankara, Turkey, and it was used as received. Methyl violet 2B (CAS number: 8004-87-3, molecular weight: 393.95 g/mol) and basic yellow 28 (CAS number 54060-92-3, molecular weight: 433.52 g/mol) were used in the adsorption experiments. Basic yellow 28, which is used in textiles with azo group, ionizes in its aqueous solutions and forms positively charged ions and is therefore a cationic dye (Slimani *et al.* 2014; Benkaddour *et al.* 2020). Methyl violet 2B, known as triphenylmethane dyes because it has 3 aryl groups attached to a nitrogen atom interacting with one or two methyl groups, is a basic dye due to the positive charge on the amino group, and its aqueous solutions are purple while the powder is dark green (Bonetto *et al.* 2015; Dahri *et al.* 2015). The chemical formulas of active pharmaceutical ingredients in black cumin thymol and the molecular structures of BY28 and MV 2B are shown in Figs. 1 and 2, respectively.

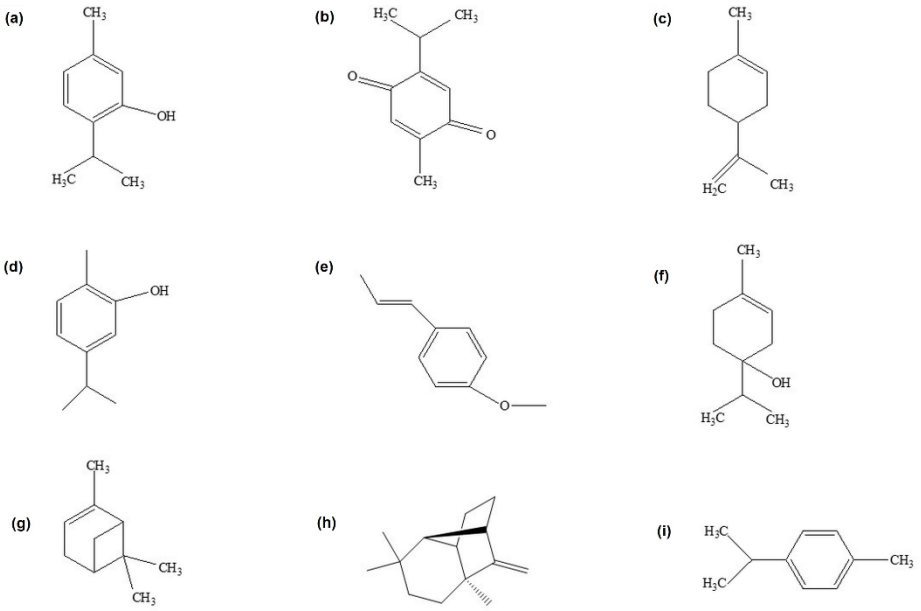

Fig. 1. Chemical formulas of active pharmaceutical ingredients in black cumin thymol (a), thymoquinone (b), limonene (c), carvacrol (d), t-anethole benzene (e), 4-terpineol (f), α-pinene (g), longifolene (h), p-simen (i) (Sismanoglu *et al.* 2022)

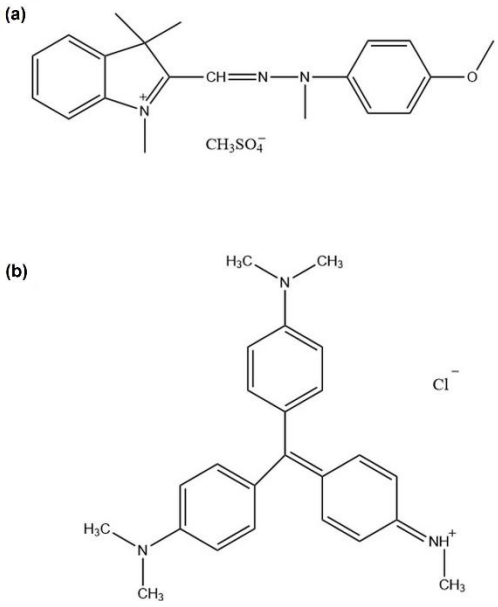

Fig. 2. Molecular structure of BY28 (a), MV (b)

Production of Biochar

The biochar was produced *via* pyrolysis of black cumin seed pulp at 500 °C with a heating rate of 10 °C/min. The pyrolysis experiments were carried out in a 250 mL stainless steel fixed bed reactor in which continuous flow of nitrogen gas was used to provide an inert atmosphere. In the pyrolysis experiment, 10 g of black cumin seeds (dry basis) was placed in the reactor. Before heating the reactor to 500 °C with a heating rate of 10 °C/min, the air inside the reactor was purged with nitrogen flow for 15 min. When the temperature reached to 500 °C, the reactor was held at that temperature for 1 h and then the heating was stopped. After cooling of the reactor to room temperature, the reactor was opened, and biochar was taken from inside the reactor. No further treatment was applied to the biochar before the adsorption experiments.

Characterization of Adsorbates and Adsorbents

The changes of adsorbates and adsorbents surfaces before and after adsorption were characterized by FTIR and SEM. In addition, thermal behavior before and after adsorption was analyzed by TGA. FTIR/ATR analysis was performed on the Alpha Bruker FTIR spectrometer, in the range of 4000 to 500 cm^{-1}, in ATR mode. SEM micrographs were taken by Carl Zeiss Ultra Plus Gemini field emission scanning electron microscope (FESEM) (Oberkochen, Germany) at a X20000 magnification. Before the experiment, the powders were covered with gold sputtering for 15 min. Thermal analysis of adsorbents and adsorbates was carried out using the Hitachi STA 7300 Thermogravimetric Analyzer in the temperature range of 25 to 600 °C in an inert nitrogen atmosphere at a heating rate of 10 ˚C/min and a nitrogen gas flow of 20 mL/min.

Batch Adsorption Experiments

Solutions of BY28 150, 100, 75, 50, 25 ppm and MV 200, 150, 100, 50, 25 ppm concentrations were made in a shaking water bath for 10, 25, 35 °C at certain intervals for a total of 60 min.

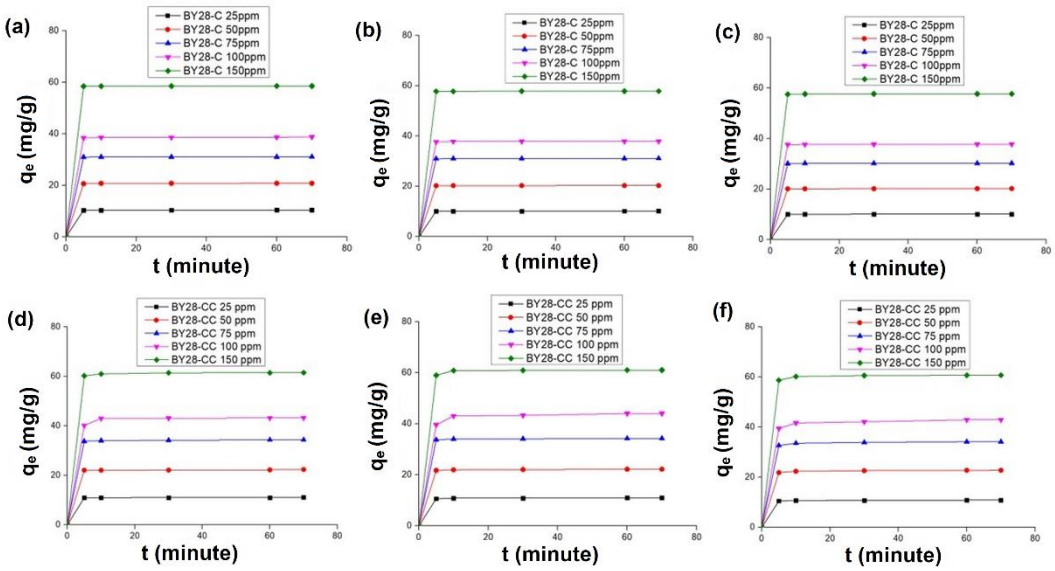

Fig. 3. Graphs of q_e (mg/g) *vs.* time of BY28-C at 10 °C (a), 25 °C (b), 35 °C (c); BY28-CC at 10 °C (d), 25 °C (e), 35 °C (f)

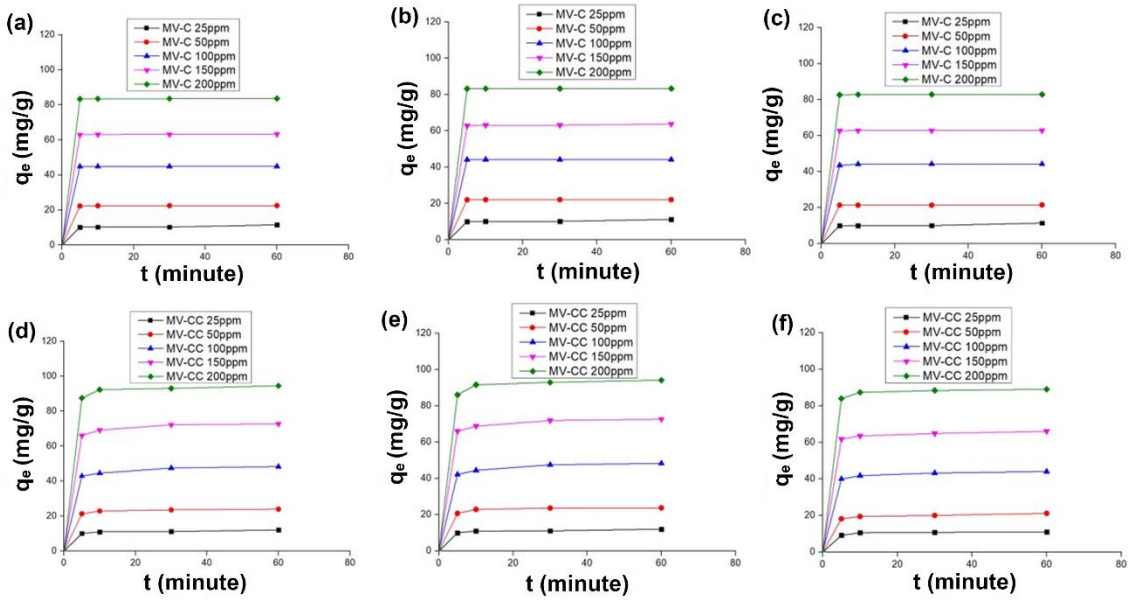

Fig. 4. Graphs of q_e (mg/g) *vs.* time of MV-C at 10 °C (a), 25 °C (b), 35 °C (c); MV-CC at 10 °C (d), 25 °C (e), 35 °C (f)

The equilibrium time of adsorption was chosen as 30 min for BY28 (Fig. 3) and 60 min for MV (Fig. 4) from the q_e *vs. t* plot. A total of 10 mL of dye concentrate, 0.02 g of black cumin, and black cumin char were used. The dose rate was 2 g/L. The pH for BY28 was 5.5 to 6, while the pH of MV was 5 to 6. The amount of dye collected on unit absorbent, q_e (mg/g), calculated as follows,

$$q_e = \frac{(c_0 - c_e)V}{m} \quad (1)$$

where c_e is the dye concentration remaining in solution after adsorption (mg/L), c_0 is the initial concentration of dye (mg/L), V is the total dye volume (L), and m is the adsorbent amount (g).

For adsorption isotherms, Freundlich, Langmuir, Temkin, Dubinin and Radushkevich (D-R), and Flory-Huggins (F-H) isotherms were used. In thermodynamic calculations, the standard Gibb's energy was calculated with the following equation (Malkoc and Nuhoglu 2007),

$$\Delta G^o = - RT \ln K_{ads} \quad (2)$$

$$K_{ads} = q_e/c_e \quad (3)$$

where K_{ads} (L/g) is the standard thermodynamic equilibrium constant. Using this equilibrium constant, with the following equation,

$$ln\ K_{ads} = - \frac{\Delta H^o}{RT} + \frac{\Delta S^o}{R} \quad (4)$$

where $\ln K_{ads}$ versus $1/T$ enthalpy from the slope of the plot provided the heat of reaction (ΔH^o kj/mol), and the entropy (ΔS^o j/molK) was obtained from the intercept with the vertical axis (Malkoc and Nuhoglu 2007; Rahchamani *et al.* 2011).

Isotherms

Freundlich

According to this isotherm, the adsorption areas on the surface of an adsorbent are heterogeneous; it is composed of different types of adsorption sites. The Freundlich isotherm equation in linear form is as follows,

$$\log q_e = \log K_F + n \log c_e \quad (5)$$

where K_F is the adsorption capacity (L/mg), and n is the adsorption density (Hakan Duran *et al.* 2019). When n<1, adsorption is favorable (Reed and Cline 1994).

Langmuir

This isotherm assumes that there are trapping points on the adsorbent surface. Assuming that each holding point will adsorb a dye molecule, the layer formed has a thickness of one molecule. In equilibrium, it reaches the maximum adsorption capacity and the surface is covered with a monolayer (Duran *et al.* 2019), as follows,

$$\frac{1}{q_e} = \frac{1}{q_{max}} + \frac{1}{q_{max}\, b\, c_e} \quad (6)$$

where q_{max} is the maximum adsorbing capacity of the adsorbent (mg/g).

Temkin

According to this isotherm, the heat of adsorption decreases linearly with the coating of the surface due to the interactions between the adsorbed dye molecules, and the participation of this heat during the adsorption will be either endothermic or exothermic (Malkoc and Nuhoglu 2007).

$$q_{e=} \frac{RT}{b_T} ln K_T + \frac{RT}{b_T} ln c_e \quad (7)$$

$$B = \frac{RT}{b_T} \quad (8)$$

$$\theta = \frac{RT}{\Delta Q_T} ln\, K_T + \frac{RT}{\Delta Q_T} ln\, c_e \quad (9)$$

where b_T is the Temkin constant (kj/molK), B is the adsorption potential (energy) related (kJ/mol), K_T is the Temkin isotherm constant (L/mg), R is the gas constant (J/molK), and θ is the ratio of the components adsorbed on the surface of the adsorbent.

The equilibrium amount (q_e mg/g) of adsorbed dyes on the surface of the adsorbent is divided by the monolayer adsorption capacity (q_{max} mg/g) from Langmuir curves. ΔQ is the adsorption energy (kJ/mol). Assuming that the process is carried out under a closed system, the heat value ΔQ is almost the same as ΔH. As a thermodynamic formula, $\Delta Q_T = - \Delta H$. The ΔH value can be defined as follows: $\Delta H > 0$ kJ/mol are endothermic processes, and $\Delta H < 0$ kJ/mol are exothermic processes (Pursell *et al.* 2011; Kireç *et al.* 2021).

Dubinin and Radushkevich (D-R)

According to this isotherm, a retained layer exhibits multi-layer character, and the following expression is used to calculate the adsorption energy of the adsorption system (Savran *et al.* 2017),

$$ln\, q_e = ln\, q_{max} - K_{D-R}\varepsilon^2 \quad (10)$$

where $K_{D\text{-}R}$ is the adsorption energy corresponding constant (mol^2kJ^2), and ε is the Pollanyi constant, calculated with $\varepsilon = RT\, ln\left(1 + \frac{1}{c_e}\right)$, and $K_{D\text{-}R}$ is the adsorption energy calculated using this formula by using the relevant constant, as shown below.

$$E = \frac{1}{\sqrt{2K_{D-R}}} \quad (11)$$

It has been stated that if this energy is within the range 8 kJ/mol < E < 16 kJ/mol, the adsorption mechanism is ionic exchange, if E < 8 kJ/mol, the adsorption mechanism is physical adsorption, and if E > 16 kJ/mol, the adsorption mechanism is diffusion (Savran *et al.* 2017).

Flory-Huggins (F-H)

While deriving the degree of coating of the surface by the dye on the adsorbent, this isotherm informs about the feasibility of the adsorption mechanism, that is, whether it is spontaneous or not (Saadi *et al.* 2015),

$$log\, \frac{\theta}{c_0} = log\, K_{F-H} + n\, log(1-\theta) \quad (12)$$

where θ is the degree of surface coverage, $K_{F\text{-}H}$ is the isotherm constant, and n is the number of ions at sorption sites. Equation 13 defines the degree of surface coverage.

$$\theta = 1 - \frac{c_e}{c_0} \quad (13)$$

The Gibb's energy is calculated using the $K_{F\text{-}H}$ constant.

$$\Delta G = -\, 2.303\, RT \log K_{F\text{-}H} \quad (14)$$

If ΔG (kj/mol) < 0, the adsorption mechanism will be spontaneous; if ΔG (kj/mol) > 0, the adsorption mechanism will not be spontaneous (Saadi *et al.* 2015).

Kinetics

Pseudo First Order Kinetic Model

The pseudo-first order kinetic model was given by Lagergren (1898) for the adsorption of solid/liquid systems and its formula is as follows,

$$\frac{dq_t}{dt} = k_1(q_e - q_t) \quad (15)$$

where k_1 is the first order adsorption rate constant (min^{-1}), q_t is the amount of substance adsorbed at time t (mgg^{-1}), and q_e is the amount of substance adsorbed (mgg^{-1}) at equilibrium. The equation with integral and boundary conditions applied is given by:

$$ln(q_e - q_t) = ln\, q_e - k_1 t \quad (16)$$

when plotting $\ln(q_e\text{-}q_t)$ versus t, the slope is k_1 (1/time).

Pseudo Second Order Kinetic Model

The basis of the second order kinetic model is based on the adsorption capacity of the solid phase (Hubbe *et al.* 2019), as follows,

$$\frac{dq_t}{dt} = k_2(q_e - q_t)^2 \quad (17)$$

where k_2 is the second order adsorption constant (g mg^{-1} min^{-1}). At t=0, q_t=0. At t=t, q_t= q_t boundary conditions are applied and equality integral is taken, as follows.

$$\frac{1}{(q_e - q_t)} = k_2 t + \frac{1}{q_e} \quad (18)$$

According to McKay and Ho the linearized form of the equation (Ho *et al.* 1999) can be expressed as,

$$\frac{t}{q_t} = \frac{1}{h} + \frac{t}{q_e} \quad (19)$$

$$h = k_2 q_e^2 \quad (20)$$

where h (mg g^{-1} min^{-1}) gives the initial sorption rate. If the graph of t/q_t *versus* t is drawn, q_e and k_2 are calculated from the slope and intercept points (Azizian 2004).

RESULTS AND DISCUSSION

FTIR/ATR Analysis Results

When the FTIR/ATR of BY28 and MV dyestuffs are examined, N-H stretching peaks in the range of 3500 to 3000 cm^{-1} and in-plane asymmetric stretching peaks of the CH_2 and CH groups are observed at 1600 cm^{-1} (Erdik 1998). The small peak seen at 2978 cm^{-1} in black seed can be attributed to the -CH band and the N-H peak (Erdik 1998; Carrión-Prieto *et al.* 2017; Thabede and Shooto 2022). The peak at 2915 cm^{-1} shows the -CH stretching in the -CH_3 and -CH_2 groups (Thabede and Shooto 2022). In the FTIR/ATR graph of black cumin char, the N-H peak disappeared after pyrolysis. The peaks between 2400 to 2300 cm^{-1} in black seed and char are C≡N stretch absorbance peaks (Durak *et al.* 2019). When BY28-C and black seed FTIR/ATR were compared, the intensity of the N-H peak between 3200 to 2800 cm^{-1} increased with the effect of the functional groups of the BY28 dyestuff. In the BY28-CC and char graphs, a new double peak is formed between 3200 to 2800 cm^{-1}, and the NH groups of the BY28 dyestuff are attached to the surface of the char. In addition, the C≡N peaks in both black seed and char intensified as the CH=N structure in BY28 penetrated the structure of black cumin and char. In the graph of BY28-CC and char FTIR/ATR, a new peak occurred in BY28-CC due to the in-plane asymmetric stretching of the CH_2 and CH groups at 1600 cm^{-1} in the structure of BY28. As with the BY28-CC, the MV-CC FTIR/ATR results are almost identical. After the adsorption of black cumin with BY28, the intensity of the peak at 1600 cm^{-1} increased. After adsorption of black seed with MV, the N-H peak of black cumin between 3200 to 2800 cm^{-1} became sharper with the penetration of the MV dyestuff. In addition, when looking at the groups present in the black cumin structure (Fig. 1); C-O tension is seen at 1064 cm^{-1}, and the aromatic extra-ring C-H bend and alkene C-H bend functional group wavelength is 668 cm^{-1} (Nandiyanto *et al.* 2019). In the BY28 dyestuff structure, it was observed that the C-

S tension of CH_3OSO_3 and the C-H and C-O groups of black cumin increased the peak intensities at 1064 cm^{-1} and 668 cm^{-1} more than the MV dye. From this, it was thought that BY28 was more adsorbed in black cumin.

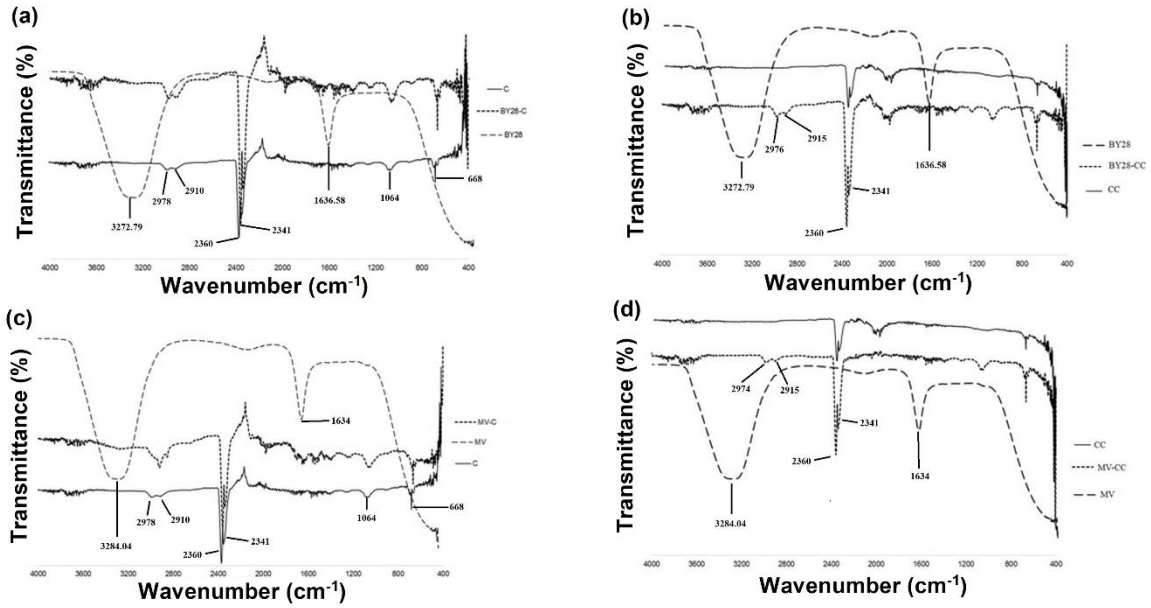

Fig. 5. FTIR/ATR spectrums of BY28-C (a), BY28-CC (b), MV-C (c), MV-CC (d)

SEM Analysis Results

Black cumin has a slotted and mounded structure, while char has a scaly and channeled structure. After the adsorption of BY28 on black cumin (Fig. 6a), the BY28 dye molecules settled into the slits and covered the surface, and the structure became smoother.

After the adsorption of MV on black cumin (Fig. 6c), a wavy structure was observed in which the dye molecules completely covered the surface, and the slits were closed. After the adsorption of char with BY28 (Fig. 6b), the surface porosity of the char increased, and the dyestuff was stuck on the surface. After adsorption with MV, channel depths were reduced by MV molecules, and its scaly structure was covered by MV (Fig. 6d). A flatter structure was formed in the adsorption of char with MV (Fig. 6d).

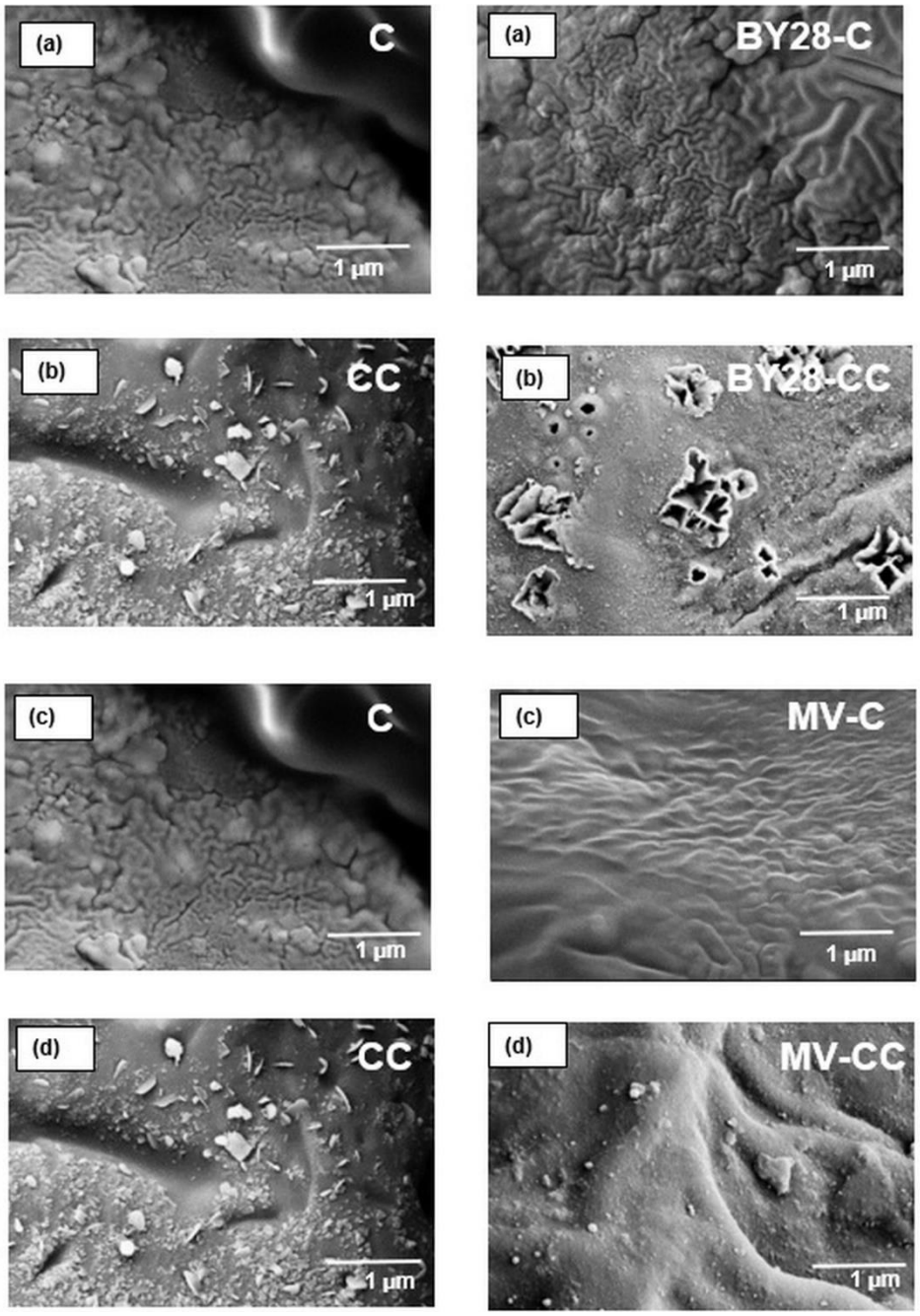

Fig. 6. Surface morphologies of BY28-C (a), BY28-CC (b), MV-C (c), MV-CC (d)

TGA Results

TGA curves for black cumin seeds and biochars before and after adsorption are shown in Fig. 7. The results were similar for black cumin seeds before and after adsorption. The evaporation of moisture was observed with the weight loss up to 135 °C. The further weight loss until 600 °C includes the thermal decomposition of hemicellulose, cellulose, and lignin. The thermal degradation of biochars was roughly similar. The evaporation of absorbed water in biochars was observed with the weight loss up to 200 °C. The weight

loss at between 200 and 450 °C can be attributed to the degradation of cellulose, hemicellulose, and other volatile components. The weight loss above that temperature reflects the degradation of residual lignin (Choudhary *et al.* 2020; Sismanoglu *et al.* 2022; Deng *et al.* 2022). When the thermal behavior graphs of the adsorption of dyestuffs with pure black cumin and pure black cumin in Figs. 7a and 7c are examined, the stages seen in the graphs are due to the impurities in the black cumin structure. In Figs. 7b and 7d, it can be seen that the impurities in black cumin decreased with pyrolysis and the temperature resistance increased in the thermal behavior graphs of the adsorption of char and char and with dyestuffs. It was observed that the weight loss (%) in the TGA curve of the adsorption experiments performed with black cumin was higher and the thermal resistance decreased accordingly. When the experiments with char were examined, it was seen that the thermal resistance values before and after adsorption were close to each other and the thermal resistance was slightly higher for both dyes after adsorption at high temperatures. These results are also consistent with the q_{max} values in Tables 1 and 2.

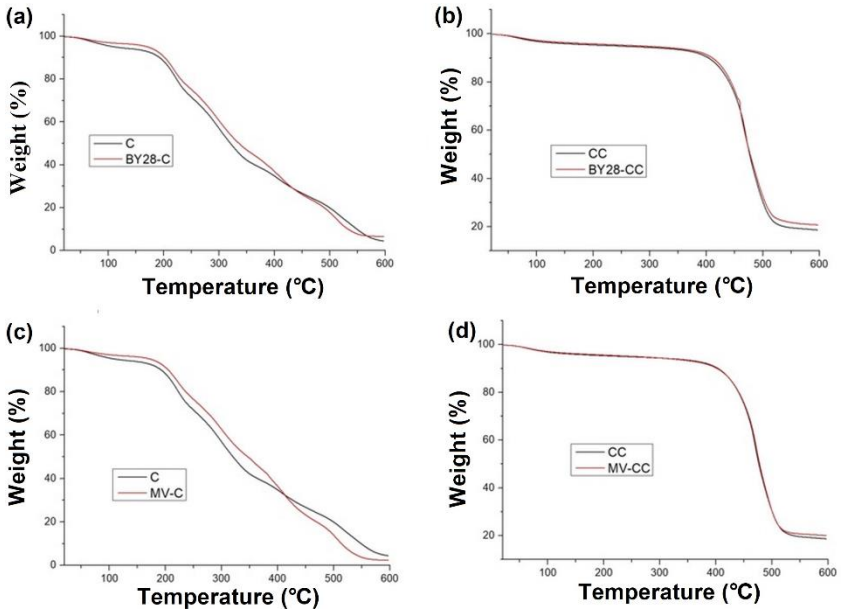

Fig. 7. TGA of BY28-C (a), BY28-CC (b), MV-C (c), MV-CC (d)

Shapes of the Isotherms

The c_e graphs (Figs. 8 and 9) drawn against q_e from the adsorption isotherm curve of both dyestuffs on the adsorbents conformed to the Giles isotherm L type. Looking at the graphs, it becomes difficult for the dye molecules to find empty space as the empty spaces on the first curve (layer) part of the adsorbent (black seed and char) are filled rapidly. Therefore, the second curve (layer) is formed. This means that a new monolayer is formed on top of the first layer (Giles *et al.* 1960). Thus, the dye molecules, rather than the solvent molecules, are more aggressively directed towards the adsorbent.

Fig. 8. Graphs of q_e (mg/g) *vs.* c_e of BY28-C at 10, 25, and 35 °C (a); BY28-CC at 10, 25, and 35 °C (b)

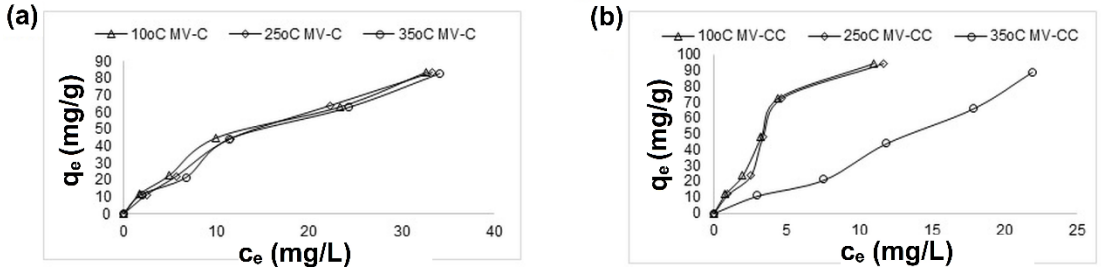

Fig. 9. Graphs of q_e (mg/g) *vs.* c_e of MV-C at 10, 25, and 35 °C (a); MV-CC at 10, 25, and 35 °C (b)

Adsorption Isotherms

K_F in the Freundlich isotherm represents the ability of adsorbates to adhere to adsorbents. K_F is the adsorption capacity in the Freundlich adsorption isotherm, and it can be meaningfully matched with q_{max} in the Langmuir isotherm. K_F has no numerical range, such that only a comparison is made of the values found as a result of the calculation. The adhesion ability of MV on black cumin was found to be higher than BY28 for all 3 temperatures (Tables 1 and 2) and K_F values for both dyes decreased with temperature. For black cumin char, the K_F was high for MV at 3 temperatures, whereas the K_F values for BY28 and MV changed irregularly with temperature. The adsorption intensity of both dyes on adsorbents was n<1, indicating that adsorption was favored. Electronegativity is the force of attraction of electrons used in bond making by the atoms forming the bond. Atoms whose external energy levels are almost completely filled, such as chlorine, are strongly electronegative and readily gain electrons. The fact that the molar mass of MV is lower than that of BY28 may cause more adhesion on the adsorbent's surface. Since the electronegativity of the Cl^- anion in the structure of the MV is high, it can be said that the adsorbent attracts the electrons on the surface more easily and the retention on the surface is therefore increased. While the compliance of BY28 to the Freundlich isotherm (R^2) of adsorption on both adsorbent at three different temperatures was between 97% and 98% for black cumin, it was between 87% and 91% for black cumin char. While the MV was between 92% and 99% for black cumin, it was between 91% and 98% for black cumin-char.

As shown in Tables 1 and 2, the q_{max} value of BY28-C for all three temperatures was quite high compared to MV-C. The q_{max} values of BY28-C and MV-C at 25 °C were 212.8 mg/g and 164 mg/g, respectively. When compared with other temperature values, it can be seen that the maximum adsorption capacity (q_{max}) of black cumin in the highest monolayer was 25 °C. The q_{max} values of black cumin char of BY28 and MV (BY28-CC,

MV-CC) at 25 °C were 625 mg/g and 909 mg/g, respectively. The q_{max} value of the char at 25 °C was higher than the values at other temperatures. According to Tables 1 and 2, the q_{max} of the BY28-C at 25 °C was higher when the MV-C was compared with the BY28-C. Likewise, when MV-CC and BY28-CC were compared according to Tables 1 and 2, the q_{max} value of MV-CC at 25 °C was higher. As a result, while the q_{max} (mg/g) data of the adsorption capacity in the Langmuir model preferred BY28 in the raw form of black cumin; it showed that the one in the char state preferred MV. While the compatibility of BY28 to the Langmuir isotherm (R^2) of adsorption on both adsorbent at three different temperatures was between 98% and 99% for black cumin, it was between 88% and 96% for black cumin-char. The suitability of MV to Langmuir isotherm (R^2) was between 96% and 99.8% for black cumin; it was between 97% and 99% for black cumin-char.

When the Temkin isotherm is applied for BY28-C, MV-C, BY28-CC, and MV-CC, the adsorption type of BY28 and MV on adsorbents is physical adsorption, since *B*, that is, the adsorption potential (energy) in the first equation of Temkin, is lower than 8 kJ/mol (Tables 1 and 2). The ΔQ adsorption energy is almost the opposite sign of the ΔH adsorption heat value result. Using the second equation of the Temkin, it was calculated that the adsorption heat of BY28 and MV dyestuffs on both adsorbent is exothermic. For black cumin and char, in which basic yellow 28 was used as dyestuff, the equivalence of the Temkin isotherm equation 7 (R^2) was between 92% and 93%, while it was between 93% and 99% for black cumin and char, respectively. When BY28 was used, the equivalence of the Temkin isotherm equation 9 (R^2) was between 93% and 95% for black cumin, while it was between 97% and 98% for black cumin char. The equivalence of MV adsorption on both adsorbent at three different temperatures to the Temkin isotherm equation 7 (R^2) is between 88% and 96% for black cumin, while it is between 86% and 94% for black cumin char. The equivalence conformity to the Temkin isotherm equation 9 (R^2) is between 91% and 96% for black cumin, and 86% to 94% for black cumin char.

Dubinin and Radushkevich (D-R) adsorption isotherm results, as shown in Tables 1 and 2 q_{max}, that is, the maximum saturation capacity for BY28-C is 41 to 42 mg/g; 42 to 53 mg/g for BY28-CC; 51 to 56 mg/g for MV-C; For MV-CC, it is 57 to 67 mg/g. Since the calculated adsorption mechanism energy (*E*) of both dyes on the adsorbents is lower than 8 kJ/mol, it is seen that physical adsorption takes place. This value is compatible with the *B* value in Temkin's first equation. The conformity of BY28 to the D-R isotherm of adsorption at three different temperatures on both adsorbent (R^2) is between 85% and 86% for black cumin, while it is between 93% and 97% for black cumin-char. The suitability of adsorption of MV on both adsorbent at three different temperatures to the D-R isotherm (R^2) is between 71% and 81% for black cumin, while it is between 75% and 82% for black cumin-char.

From the Flory-Huggins (F-H) adsorption isotherm results for BY28-C, BY28-CC, MV-C, and MV-CC, (Tables 1 and 2), $\log K_{F\text{-}H}$ was positive as a result of adsorption of both dyes on black cumin and char, and the adsorption reaction energy was calculated from Eq. 14 as ΔG kj/mol < 0. The adsorption of both dyes on black cumin and black cumin-char was spontaneous.

Table 1. Isotherms Data of BY28-C and BY28-CC

BY28-C								
***t*/°C**	**Freundlich**			**Langmuir**				
	n	K_F	R^2	q_{max}	K_L	R^2		
10	0.78	3.71	0.98	169.5	0.0158	0.99		
25	0.84	2.93	0.98	212.8	0.0107	0.99		
35	0.84	2.87	0.98	204.1	0.011	1		
	Temkin							
	b_T	R^2	K_T(L/mg)	H(kJ/mol)	R^2			
10	0.108	0.94	0.34	-18.6	0.95			
25	0.11	0.93	0.31	-23.4	0.93			
35	0.114	0.93	0.28	-23.3	0.93			
BY28-CC								
***t*/°C**	**Freundlich**			**Langmuir**				
	n	K_F	R^2	q_{max}	K_L	R^2		
10	0.73	6.17	0.91	357	0.0114	0.96		
25	0.73	6.12	0.9	625	0.0065	0.94		
35	0.7	6.38	0.87	556	0.007	0.9		
	Temkin							
	b_T	R^2	K_T(L/mg)	H(kj/mol)	R^2			
10	0.105	0.97	0.56	-37.8	0.97			
25	0.114	0.99	0.55	-69.5	0.98			
35	0.12	0.97	0.56	-67	0.97			
BY28-C								
***t*/°C**	**D-R**				**F-H**			
	K_{DR}	q_{max}	E(kJ/mol)	R^2	n	logK_{FH}	G(kJ/mol)	R^2
10	5.88	42.2	0.29	0.86	4.23	1.14	-6.19	0.83
25	6.67	41.7	0.27	0.86	5.39	1.768	-10.1	0.86
35	6.74	41.3	0.27	0.85	5.51	1.8125	-10.7	0.85
BY28-CC								
***t*/°C**	**D-R**				**F-H**			
	K_{DR}	q_{max}	E(kJ/mol)	R^2	n	logK_{FH}	G(kJ/mol)	R^2
10	2.89	42.5	0.42	0.93	2.66	0.525	-2.85	0.98
25	3.89	53	0.36	0.97	2.48	0.38	-2.16	0.98
35	3.18	51.2	0.4	0.95	2.22	0.073	-0.423	0.93

Table 2. Isotherms Data of MV-C and MV-CC

MV-C								
***t*/°C**	**Freundlich**			**Langmuir**				
	n	K_F	R^2	q_{max}	K_L	R^2		
10	0.67	8.17	0.98	96.2	0.077	0.99		
25	0.77	5.86	0.99	164	0.029	1		
35	0.7	3.06	0.93	86	0.075	0.97		
	Temkin							
	b_T	R^2	K_T(L/mg)	H(kJ/mol)	R^2			
10	0.098	0.89	0.72	-9.42	0.95			
25	0.089	0.96	0.49	-14.5	0.96			
35	0.103	0.91	0.58	-8.9	0.91			
MV-CC								
***t*/°C**	**Freundlich**			**Langmuir**				
	n	K_F	R^2	q_{max}	K_L	R^2		
10	0.84	15.6	0.94	303	0.051	0.99		
25	0.89	13	0.91	909	0.0132	0.98		
35	1	9.58	0.98	625	0.006	0.98		
	Temkin							
	b_T	R^2	K_T(L/mg)	H(kJ/mol)	R^2			
10	0.07	0.93	1.46	-21	0.94			
25	0.07	0.91	1.17	-62	0.91			
35	0.07	0.88	0.34	-42.7	0.86			
MV-C								
***t*/°C**	**D-R**				**F-H**			
	K_{DR}	q_{max}	E(kJ/mol)	R^2	n	logK_{FH}	G(kJ/mol)	R^2
10	1.46	54.2	0.58	0.79	2.36	0.274	-1.49	0.89
25	2.78	56.6	0.43	0.81	4.06	1.67	-9.5	0.97
35	1.74	51.6	0.54	0.7	2.6	0.35	-2.04	0.83
MV-CC								
***t*/°C**	**D-R**				**F-H**			
	K_{DR}	q_{max}	E(kj/mol)	R^2	n	logK_{FH}	G(kJ/mol)	R^2
10	0.51	67.2	1	0.82	3.31	2.81	-15.2	0.94
25	0.8	67.6	0.84	0.8	3.18	2.46	-14	0.98
35	3.87	57.5	0.36	0.75	6	3.51	-21	0.81

The conformity of BY28 adsorption to the F-H isotherm (R^2) of adsorption on both adsorbent at three different temperatures is between 83% and 86% for black cumin, while it is between 93% and 98% for black cumin-char. The suitability of adsorption of MV on both adsorbent at three different temperatures to the F-H isotherm (R^2) is between 82% and 96.5% for black cumin, while it is between 80% and 98.5% for black cumin-char.

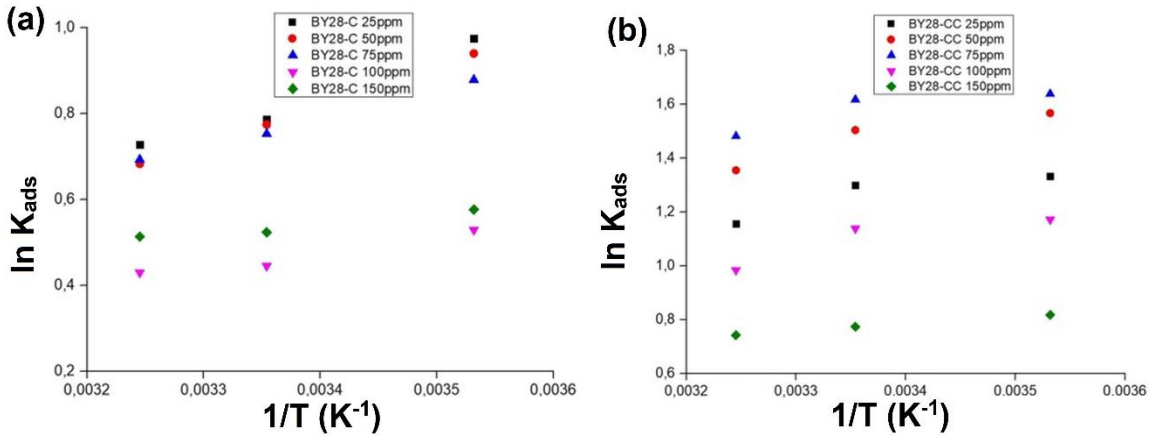

Fig. 10. Graphs of lnK_{ads} *vs.* 1/T(K^{-1}) of BY28-C (a); BY28-CC (b)

Using the thermodynamic values according to the data obtained from the adsorption experiments with BY28 and MV dyes; $K_{ads} = q_e/c_e$ (L/g) using the standard thermodynamic equilibrium constant with the following equation; $\ln K_{ads} = -\frac{\Delta G^{\circ}}{RT} = -\frac{\Delta H^{\circ}}{RT} + \frac{\Delta S^{\circ}}{R}$. Enthalpy ($\Delta H^{o}$ kJ/mol) was calculated from the slope of the graph plotted against lnK_{ads} versus 1/T, and entropy (ΔS^{o} J/molK) was calculated from the cutoff point. And the Gibbs free energy (ΔG^{o} kJ/mol) value was also calculated from the equation. Looking at the graph 10 and Table 3 for BY28-C and BY28-CC, the adsorption energy (ΔH^{o}) indicates that it was an exothermic reaction. The entropy value was negative. This shows that the dye was adsorbed on black cumin and black cumin char, that is, it changed from an irregular state to a regular state.

Table 3. Thermodynamics Data of BY28-C (a); BY28-CC (b)

BY28-C					
c_o/ppm	**(10 °C-35 °C)**	**(10 °C-35 °C)**	**10 °C**	**25 °C**	**35 °C**
	***H*(kJ/mol)**	***S*(J/molK)**	***G*(kJ/mol)**	***G*(kJ/mol)**	***G*(kJ/mol)**
25	-7.33	-17.9	-2.3	-2	-1.8
50	-7.48	-18.6	-2.2	-1.93	-1.7
75	-5.44	-11.9	-2.1	-1.89	-1.8
100	-2.98	-6.17	-1.2	-1.14	-1.1
150	-1.88	-1.9	-1.4	-1.32	-1.3
BY28-CC					
c_o/ppm	**(10 °C-35 °C)**	**(10 °C-35 °C)**	**10 °C**	**25 °C**	**35 °C**
	***H*(kJ/mol)**	***S*(J/molK)**	***G*(kJ/mol)**	***G*(kJ/mol)**	***G*(kJ/mol)**
25	-4.75	-5.56	-3.2	-3.09	-3
50	-5.85	-7.48	-3.7	-3.62	-3.5
75	-4.23	-1.14	-3.9	-3.89	-3.9
100	-5.07	-8	-2.8	-2.67	-2.6
150	-2.18	-0.88	-1.9	-1.91	-1.9

Gibbs free energy values were negative. This means that the adsorption was spontaneous. For MV-C and MV-CC, the adsorption energy (ΔH^o) indicates that it was an exothermic reaction. The entropy value of MV-C was negative between 25 and 150 ppm, but this value was calculated to be positive at 200 ppm. The entropy value of MV-CC was negative within the range 25 to 100 ppm, but this value was calculated to be positive at 150 to 200 ppm. Here, the negative value of ΔS^o indicates that the dye changed from an irregular state to a regular state on black cumin and black cumin char. Gibbs free energy values were negative. This indicates that the adsorption is spontaneous. The ΔG values obtained from the thermodynamic calculations and the ΔG values obtained from the Flory-Huggins (F-H) adsorption isotherm were compatible with each other.

Table 4. Thermodynamics Data of MV-C (a); MV-CC (b)

MV-C					
c_0/ppm	**(10 °C-35 °C)**	**(10 °C-35 °C)**	**10 °C**	**25 °C**	**35 °C**
	***H*(kJ/mol)**	***S*(J/molK)**	***G*(kJ/mol)**	***G*(kJ/mol)**	***G*(kJ/mol)**
25	-11	-22.4	-4.51	-4.18	-3.95
50	-10	-23.9	-3.62	-3.26	-3.02
100	-4.8	-4.6	-3.29	-3.43	-3.38
150	-2.8	-1.09	-2.47	-2.45	-2.44
200	-1.5	254	-2.21	-2.25	-2.27
MV-CC					
c_0/ppm	**(10 °C-35 °C)**	**(10 °C-35 °C)**	**10 °C**	**25 °C**	**35 °C**
	***H*(kJ/mol)**	***S*(J/molK)**	***G*(kJ/mol)**	***G*(kJ/mol)**	***G*(kJ/mol)**
25	-12	-19.4	-6.41	-6.12	-5.93
50	-10	-15.4	-5.83	5.59	-5.44
100	-12	-18.5	-6.39	-6.11	-5.93
150	-3.3	11.7	-6.57	-6.75	-6.87
200	-3.8	4.63	-5.07	-5.14	-5.18

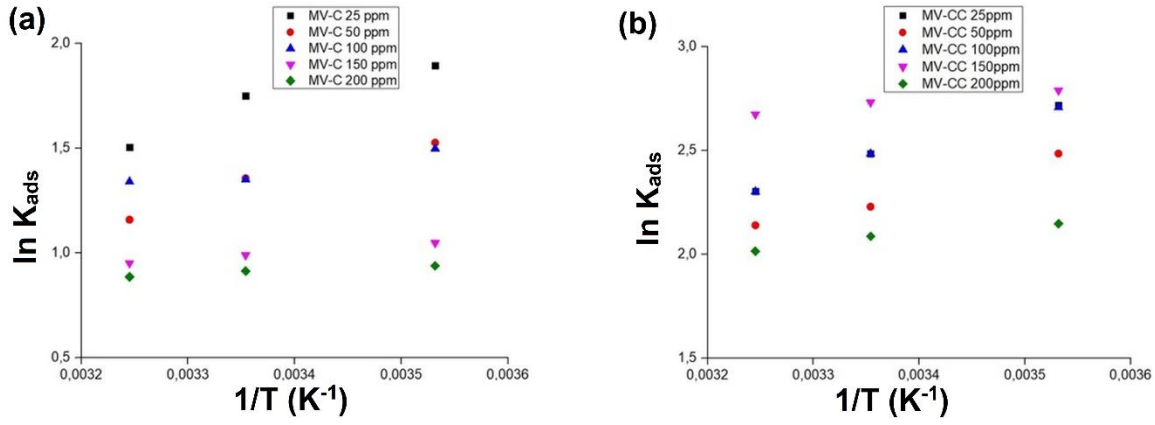

Fig. 11. Graphs of lnK_{ads} *vs.* 1/T(K^{-1}) of MV-C (a); MV-CC (b)

Adsorption Kinetics

The kinetic studies of BY28 and MV dyestuffs on both adsorbents at five different concentrations and three different temperatures were fitted to pseudo-first-order and pseudo-second-order rate equations. Rate graphs were drawn for 25 °C, where both dyestuffs were adsorbed the most on the adsorbents, and rate constants and q_e values are shown in the Tables 5 and 6. When the experimentally found q_e value and the theoretically calculated q_e values in Table 5 and 6 were compared, the best value fit the pseudo-second-order velocity equation. In addition, the degree of fit R^2 was close to 100% with the pseudo-second order velocity equation.

Table 5. Kinetic Data of BY28-C (a); BY28-CC (b)

BY28-CC		pseudo-first order			pseudo-second order		
c_o/ppm	q_e,exp(mg/g)	k_1(1/min)	q_e,calc(mg/g)	R^2	k_2(g/mg min)	q_e,calc(mg/g)	R^2
10 °C							
25	**11.06**	0.077	0.67	0.5	1.22	**11.08**	1
50	**22.38**	0.05	1.66	0.4	0.29	**22.37**	1
75	**34.38**	0.083	2.98	0.6	0.23	**34.48**	1
100	**43.28**	0.082	4.72	0.6	0.09	**43.47**	1
150	**61.47**	0.119	5.24	0.8	0.26	**61.72**	1
25 °C							
25	**10.97**	0.074	1.05	0.6	0.55	**10.99**	1
50	**22.22**	0.08	2.13	0.6	0.31	**22.27**	1
75	**34.25**	0.11	3.26	0.8	0.28	**34.25**	1
100	**44.02**	0.122	13.2	0.9	0.03	**44.25**	1
150	**61.04**	0.13	5.94	0.8	0.15	**60.97**	1
35 °C							
25	**10.89**	0.101	1.26	0.8	0.42	**10.92**	1
50	**22.78**	0.088	3.22	0.8	0.19	**22.83**	1
75	**34.17**	0.126	7.12	0.9	0.11	**34.24**	1
100	**42.93**	0.12	13.2	0.9	0.05	**43.29**	1
150	**60.71**	0.116	7.21	0.8	0.12	**60.97**	1
BY28-C		pseudo-first order			pseudo-second order		
c_o/ppm	q_e,exp(mg/g)	k_1(1/min)	q_e,calc(mg/g)	R^2	k_2(g/mg min)	q_e,calc(mg/g)	R^2
10 °C							
25	**10.42**	0.118	0.62	0.7	2.04	**10.44**	1
50	**20.83**	0.079	0.82	0.5	1.21	**20.83**	1
75	**31.09**	0.083	0.87	0.4	1.29	**31.1**	1
100	**38.79**	0.057	1.7	0.3	0.42	**38.76**	1
150	**58.56**	0.096	1.11	0.5	1.46	**57.47**	1
25 °C							
25	**10.17**	0.072	0.47	0.5	1.58	**10.17**	1
50	**20.31**	0.108	0.64	0.6	2.42	**20.33**	1
75	**31.09**	0.118	0.51	0.5	3.61	**30.4**	1
100	**37.88**	0.091	1	0.5	1.16	**37.87**	1
150	**57.86**	0.116	1.21	0.5	1.48	**57.8**	1
35 °C							
25	**10.12**	0.093	0.37	0.5	3.05	**10.12**	1
50	**20.24**	0.069	0.85	0.4	0.98	**20.24**	1
75	**30.26**	0.06	0.71	0.3	1.57	**30.21**	1
100	**37.78**	0.07	1.15	0.4	0.88	**37.73**	1
150	**57.73**	0.117	1.16	0.6	1.5	**57.8**	1

Table 6. Kinetic Data of MV-C (a); MV-CC (b)

MV-CC		pseudo-first order			pseudo-second order		
c_o/ppm	q_e,exp (mg/g)	k_1 (1/min)	q_e,calc (mg/g)	R^2	k_2 (g/mg min)	q_e,calc (mg/g)	R^2
10°C							1
25	**12.1**	0.086	5.51	0.89	0.08	**12.34**	1
50	**24**	0.087	6.69	0.89	0.099	**24.4**	1
100	**48.36**	0.13	22.18	0.96	0.036	**49.89**	1
150	**72.76**	0.142	27.19	0.96	0.043	**76.92**	1
200	**94.48**	0.121	25.74	0.89	0.05	**100**	1
25 °C							
25	**12**	0.089	5.595	0.89	0.082	**12.19**	1
50	**23.73**	0.114	6.638	0.90	0.112	**24.39**	1
100	**48.3**	0.065	14.85	0.81	0.033	**50**	1
150	**72.63**	0.144	29.76	0.96	0.034	**77**	1
200	**94.15**	0.133	30.14	0.92	0.033	**100**	1
35 °C							
25	**11**	0.089	3.27	0.86	0.172	**11.11**	1
50	**21.19**	0.118	11.3	0.91	0.057	**21.74**	1
100	**44.06**	0.123	16.52	0.93	0.054	**45.45**	1
150	**66.06**	0.126	21.11	0.91	0.056	**66.66**	1
200	**89.04**	0.137	22.04	0.91	0.061	**90.9**	1
MV-C		pseudo-first order			pseudo-second order		
c_o/ppm	q_e,exp (mg/g)	k_1 (1/min)	q_e,calc (mg/g)	R^2	k_2 (g/mg min)	q_e,calc (mg/g)	R^2
10 °C							
25	**11.63**	0.108	6.53	0.86	0.072	**11.76**	1
50	**22.55**	0.111	0.864	0.62	2.23	**22.73**	1
100	**44.97**	0.074	1.12	0.4	1.51	**45.45**	1
150	**63.27**	0.104	2.44	0.6	0.83	**62.5**	1
200	**83.64**	0.106	2.83	0.6	0.78	**83.33**	1
25 °C							
25	**11.25**	0.07	4.19	0.8	0.088	**11.37**	1
50	**22.15**	0.082	0.5	0.4	3.42	**22.15**	1
100	**44.22**	0.092	0.82	0.5	2.83	**44.22**	1
150	**63.81**	0.11	8.08	0.8	0.15	**63.86**	1
200	**83.29**	0.1	1.45	0.5	2.02	**83.3**	1
35 °C							
25	**11.5**	0.098	6.3	0.86	0.065	**11.63**	1
50	**21.6**	0.093	1.59	0.65	0.705	**21.73**	1
100	**42.3**	0.122	2.21	0.65	0.638	**44.31**	1
150	**62.9**	0.105	1.28	0.5	2.15	**62.87**	1
200	**82.9**	0.114	1.86	0.6	1.44	**83.33**	1

It was reported that good fits to the pseudo-second-order rate equations tend to indicate that the rate of adsorption is governed by diffusion of dye molecules within a network of very small pores (Hubbe *et al*. 2019). In conclusion, at 25-50-75-100-150 ppm concentrations, it was observed that BY28 satisfies the adsorption kinetic pseudo-second-order rate equation 100% for temperatures of 10-25-35 °C on black cumin and black

cumin-char. In addition to these results; at 25-50-100-150-200 ppm concentrations, it was observed that the adsorption kinetics of MV on black cumin and black cumin-char at 10-25-35 °C complied with the pseudo-second-order velocity equation 100%.

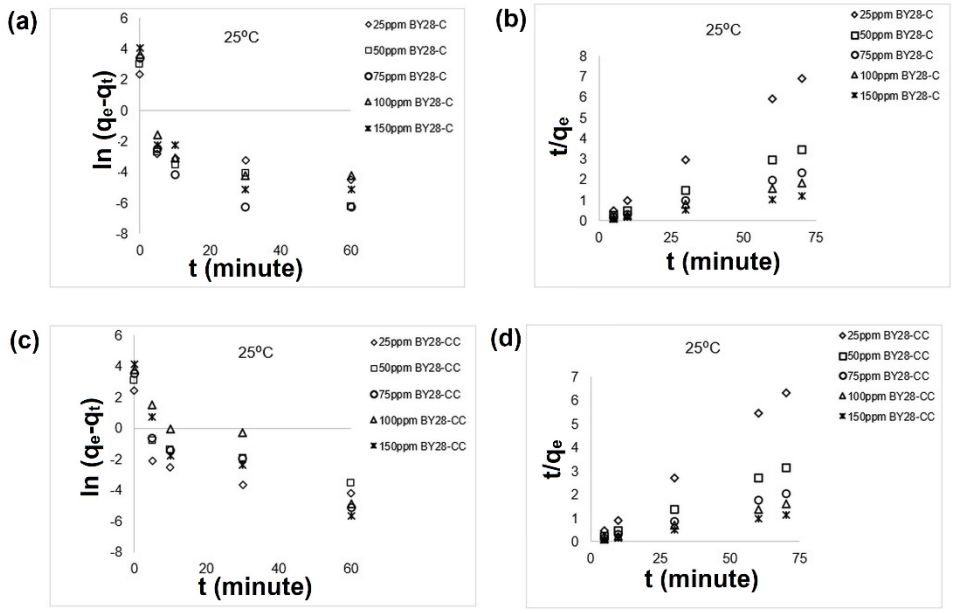

Fig. 12. Graphs of ln (q_e-q_t) *vs. t*(min) of BY28-C (a), BY28-CC (c); Graphs of t/q_e *vs. t* (min) of BY28-C (b), BY28-CC (d)

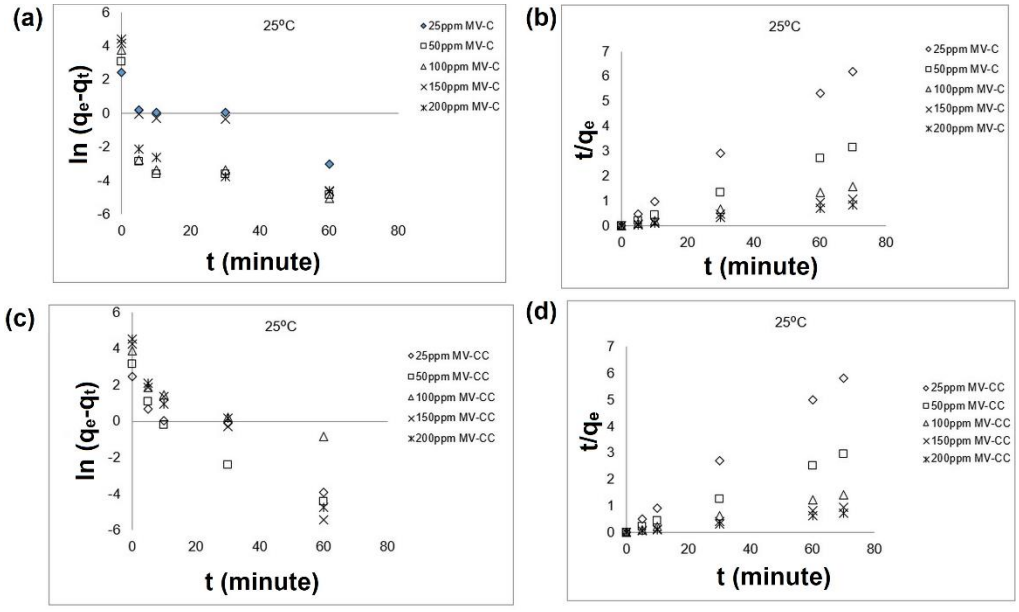

Fig. 13. Graphs of ln (q_e-q_t) *vs. t*(min) of MV-C (a), MV-CC (c); Graphs of t/q_e *vs. t* (min) of MV-C (b), MV-CC (d)

CONCLUSIONS

1. The Freundlich adsorption capacity (K_F; L/mg) constant was higher for biochar produced from cumin seed (CC), was shown in Tables 1 and 2. These findings are based on adsorption experiments carried out with basic yellow 28 (BY28) and methyl violet (MV).
2. Adsorption potential (energy) values *B* obtained from the Temkin isotherm, as well as heat of adsorption values *E* obtained from Dubinin-Radushkevich (D-R) isotherm, for both dyes were smaller than 8 kJ/mol for three different temperatures on the adsorbents. These results imply that the adsorption took place by physical adsorption.
3. When the heat of adsorption ΔH^o calculated from the Temkin isotherm was compared with the heat of adsorption calculated from the thermodynamic calculation, ΔH, it was exothermic for all adsorption systems. The results of both values supported each other.
4. When the Gibbs energy ΔG^o calculated from the F-H isotherm was compared with the standard Gibbs energy ΔG found from the thermodynamic calculation, the adsorption reaction was spontaneous for BY28-C, BY28-CC, MV-C, and MV-CC. The results of both values supported each other.
5. For all three temperatures, when the sorbent dose was 2 g/L (V=10 mL, m=0.02 g), its adsorption on black cumin and black cumin-char adsorbents reached equilibrium within 30 min for BY28 dyestuff, while it reached equilibrium in 60 min for MV dyestuff. As a result of adsorption, the pH value of BY28 was determined as 7 and that of MV as 8. Langmuir q_{max} of BY28 was found as 625 mg/g on black seed-char and 212 mg/g on black seed for 25 °C. Langmuir q_{max} of MV was 909 mg/g on black seed-char and 164 mg/g on black seed for 25 °C. Thus, both black cumin and black cumin-char are expected to be very effective in removing BY28 and MV from wastewater due to its short, required retention time and high amount of adsorption on the adsorbent.

ACKNOWLEDGMENTS

The authors thank emeritus Prof. Dr. Tuba Şişmanoğlu for her experience and knowledge.

REFERENCES CITED

Akdemir, M., Isik, B., Cakar, F., and Cankurtaran, O. (2022). "Comparison of the adsorption efficiency of cationic (Crystal Violet) and anionic (Congo Red) dyes on Valeriana officinalis roots: Isotherms, kinetics, thermodynamic studies, and error functions," *Mater. Chem. and Phys.* 291, ID: 126763. DOI: 10.1016/j.matchemphys.2022.126763

Ariani, D., Aprilita, N. H., and Kuncaka, A. (2018). "Adsorption of Malachite Green and Methyl Violet 2B with phthalate-functionalized sugarcane bagasse," *BIMIPA* 25(1), 66-79.

Astuti, W., and Fatin, D. M. (2018). "Adsorption of methyl violet dye by thermally modified ceiba pentandra sawdust," *Jurnal Bahan Alam Terbarukan* 6(2), 183-189. DOI: 10.15294/jbat.v6i2.12126

Azizian, S. (2004). "Kinetic models of sorption: A theoretical analysis," *J. Colloid Interf. Sci.* 276(1), 47-52. DOI: 10.1016/j.jcis.2004.03.048

Bader, A. T. (2019). "Removal of Methyl Violet (MV) from aqueous solutions by adsorption using activated carbon from pine husks (Plant Waste Sources)," *Plant Arch.* 19(2), 898-901.

Benkaddour, S., El Ouahabi, I., Hiyane, H., Essoufy, M., Driouich, A., El Antri, S., El Hajjaji, S., Slimani, R., and Lazar, S. (2020). "Removal of Basic Yellow 28 by biosorption onto watermelon seeds, part I: The principal factors influencing by Plackett-Burman screening design," *Surfaces and Interfaces* 21, article 100732. DOI: 10.1016/j.surfin.2020.100732

Bonetto, L.R., Ferrarini, F., De Marco, C., Crespo, J.S., Gu´egan, R., and Giovanela, M. (2015) "Removal of methyl violet 2B dye from aqueous solution using a magnetic composite as an adsorbent," *J. Water Process. Eng.* 6, 11-20. DOI: 10.1016/j.jwpe.2015.02.006

Can, M. (2020). "Determination of producer behaviors, problems and solutions in cultivation of black cumin: Example of Uşak province," *Ziraat Mühendisliği* 370, 18-33. DOI: 10.33724/zm.744575

Carrión-Prieto, P., Silva-Castro, I., Ramos-Silva, M., Martín-Ramos, P., Martín-Gil, J., and Hernández-Navarro, S. (2017). "Vibrational analysis and thermal behavior of *Salvia hispanica*, *Nigella sativa* and *Papaver somniferum* seeds," *Pharmacogn J.* 9(2), 157-162 (No. ART-2017-99182). DOI: 10.5530/pj.2017.2.26

Choi, J., Won, W., and Capareda, S. C. (2019). "The economical production of functionalized Ashe juniper derived-biochar with high hazardous dye removal efficiency," *Ind. Crop. Prod.* 137, 672-680. DOI: 10.1016/j.indcrop.2019.05.006

Choudhary, M., Kumar, R., and Neogi, S. (2020). "Activated biochar derived from Opuntia ficus-indica for the efficient adsorption of malachite green dye, Cu^{+2} and Ni^{+2} from water," *J. Hazard. Mater.* 392, ID: 122441. DOI: 10.1016/j.jhazmat.2020.122441

Dahri, M. K., Kooh, M. R. R., and Lim, L. B. (2013). "Removal of methyl violet 2B from aqueous solution using Casuarina equisetifolia needle," *International Scholarly Research Notices* 2013, ID: 619819. DOI: 10.1155/2013/619819

Dahri, M. K., Chieng, H. I., Lim, B. L. L., Priyantha, N., and Mei, C. C. (2015). "Cempedak durian (*Artocarpus* sp.) peel as a biosorbent for the removal of toxic methyl violet 2B from aqueous solution," *Korean Chem. Eng. Res.* 53(5), 576-583. DOI: 10.9713/kcer.2015.53.5.576

Dao, S. D., Nguyen, B., and Tran, T. H. T. (2013). "Adsorption of basic yellow 28 in aqueous solution by activated carbon," *Asian J. Chem.* 25(4), 2173-2176. DOI: 10.14233/ajchem.2013.13381

Deng, H., Li, Y. F., Tao, S. Q., Li, A. Y., and Li, Q. Y. (2022). "Efficient adsorption capability of banana and cassava biochar for malachite green: Removal process and mechanism exploration," *Environmental Engineering Research* 27(3). DOI: 10.4491/eer.2020.575

Durak, H., Genel, S., and Tunç, M. (2019). "Pyrolysis of black cumin seed: Significance of catalyst and temperature product yields and chromatographic characterization," *J. Liq. Chromatog. R. T.* 42(11-12), 331-350. DOI: 10.1080/10826076.2019.1593194

Duran, H., Sismanoglu, S., and Sismanoglu, T. (2019). "Binary biomaterials (inorganic material/natural resin): synthesis, characterization and performance for adsorption of dyes," *J. Ind. Chem. Soc.* 96, 1245-1251.

Erdik, E. (1998). *Organik Kimyada Spektroskopik Yöntemler*. Gazi Kitabevi, Ankara.

Erdogan, Y., Isik, B., Ugraskan, V., and Cakar, F. (2022). "Effective and fast removal of crystal violet dye from aqueous solutions using *Rumex acetosella*: Isotherm, kinetic, thermodynamic studies, and statistical analysis," *Biomass Conversion and Biorefinery* 1-16. DOI: 10.1007/s13399-022-02349-9

Giles, C. H., MacEwan, T. H., Nakhwa, S. N., and Smith, D. (1960). "A system of classification of solution adsorption isotherms, and its use in diagnosis of adsorption mechanisms and in measurement of specific surface areas of solids," *J. Chem. Soc* 111, 3973-3993. DOI: 10.1039/jr9600003973

Han, X., Chu, L., Liu, S., Chen, T., Ding, C., Yan, J., Cui, L., and Quan, G. (2015). "Removal of methylene blue from aqueous solution using porous biochar obtained by KOH activation of peanut shell biochar," *BioResources* 10(2), 2836-2849. DOI: 10.15376/biores.10.2.2836-2849

Ho, Y. S., and McKay, G. (1999). "Pseudo-second order model for sorption processes," *Process Biochem.* 34(5), 451-465. DOI: 10.1016/S0032-9592(98)00112-5

Hubbe, M. A., Azizian, S., and Douven, S. (2019). "Implications of apparent pseudo-second-order adsorption kinetics onto cellulosic materials. A review," *BioResources* 14(3), 7582-7626. DOI: 10.15376/biores.14.3.7582-7626

Isik, B., Ugraskan, V., Cakar, F., and Yazici, O. (2022) "A comparative study on the adsorption of toxic cationic dyes by Judas tree (*Cercis siliquastrum*) seeds," *Biomass Conversion and Biorefinery* 1-15. DOI: 10.1007/s13399-022-02679-8

Kalpaklı, Y., Toygun, Ş., Köneçoğlu, G., and Akgün, M. (2014). "Equilibrium and kinetic study on the adsorption of basic dye (BY28) onto raw Ca-bentonite," *Desalin. Water Treat.* 52(37-39), 7389-7399. DOI: 10.1080/19443994.2013.830804

Karadeniz, S. C., Isik, B., Ugraskan, V., and Cakar, F. (2023). "Agricultural *Lolium perenne* seeds as a low-cost biosorbent for Safranine T adsorption from wastewater: Isotherm, kinetic, and thermodynamic studies," *Phys. Chem. Earth* 129, ARTICLE ID: 103338. DOI: 10.1016/j.pce.2022.103338

Kireç, O., Alacabey, İ., Erol, K., and Alkan, H. (2021). "Removal of 17β-estradiol from aqueous systems with hydrophobic microspheres," *J. Polym. Eng.* 41(3), 226-234. DOI: 10.1515/polyeng-2020-0150

Koşar, İ., and Özel, A. (2018). "Çörekotu (Nigella sativa L.) çeşit ve popülasyonlarının karakterizasyonu: Tarımsal özellikler." *Harran Tarım ve Gıda Bilimleri Dergisi,* 22(4), 533-543. DOI: 10.29050/ harranziraat.399540

Lagergren, S. (1898). "Zur theorie der sogenannten adsorption geloster stoffe. Kungliga svenska vetenskapsakademiens," *Handlingar* 24, 1-39.

Malkoc, E., and Nuhoglu, Y. (2007). "Determination of kinetic and equilibrium parameters of the batch adsorption of Cr (VI) onto waste acorn of *Quercus ithaburensis*," *Chemical Engineering and Processing-Process Intensification* 46(10), 1020-1029. DOI: 10.1016/j.cep.2007.05.007

Nandiyanto, A. B. D., Oktiani, R., and Ragadhita, R (2019). "How to read and interpret FTIR spectroscope of organic material," *Indones. J. Sci. Technol.* 4(1), 97-118. DOI: 10.17509/ijost.v4i1.15806

Pursell, C. J., Hartshorn, H., Ward, T., Chandler, B. D., and Boccuzzi, F. (2011). "Application of the Temkin model to the adsorption of CO on gold," *J. Phys. Chem. C* 115(48), 23880-23892. DOI: 10.1021/jp207103z

Rahchamani, J., Mousavi, H. Z., and Behzad, M. (2011). "Adsorption of methyl violet from aqueous solution by polyacrylamide as an adsorbent: Isotherm and kinetic studies," *Desalination* 267(2-3), 256-260. DOI: 10.1016/j.desal.2010.09.036

Reed, B. E., and Cline, S. R. (1994). "Retention and release of lead by a very fine sandy loam. I. Isotherm modeling," *Sep. Sci. Technol.* 29(12), 1529-1551. DOI: 10.1080/01496399408007372

Regti, A., Laamari, M. R., Stiriba, S. E., and El Haddad, M. (2017). "Potential use of activated carbon derived from *Persea* species under alkaline conditions for removing cationic dye from wastewaters," *Journal of the Association of Arab Universities for Basic and Applied Sciences* 24, 10-18. DOI: 10.1016/j.jaubas.2017.01.003

Saadi, R., Saadi, Z., Fazaeli, R., and Fard, N. E. (2015). "Monolayer and multilayer adsorption isotherm models for sorption from aqueous media," *Korean J. Chem. Eng.* 32, 787-799. DOI: 10.1007/s11814-015-0053-7

Savran, A., Selçuk, N., Kubilay, Ş., and Kul, A. (2017). "Adsorption isotherm models for dye removal by paliurus spinachristi mill. frutis and seeds in a single component system," *IOSR J. Environ. Sci. Toxicol. Food Technol*. 11(04), 18-30. DOI: 10.9790/2402-1104021830

Singh, M., Ahsan, M., Pandey, V., Singh, A., Mishra, D., Tiwari, N., Singh, P., Karak, T., and Khare, P. (2022). "Comparative assessment for removal of anionic dye from water by different waste-derived biochar vis a vis reusability of generated sludge," *Biochar* 4(1), 13. DOI: 0.1007/s42773-022-00140-7

Sismanoglu, S., Tayfun, Ü., Gradinariu, P., Popescu, C. M., and Kanbur, Y. (2022). "Reuse of black cumin biomass into beneficial additive for thermoplastic polyurethane-based green composites with silane modifiers," *Biomass Conversion and Biorefinery* 1-16. DOI: 10.1007/s13399-022-03023-w

Slimani, R., El Ouahabi, I., Abidi, F., El Haddad, M., Regti, A., Laamari, M. R., El Antri, S., and Lazar, S. (2014). "Calcined eggshells as a new biosorbent to remove basic dye from aqueous solutions: thermodynamics, kinetics, isotherms and error analysis," *J. Taiwan Inst. Chem. Eng*. 45(4), 1578-1587. DOI: 10.1016/j.jtice.2013.10.009

Temiz, R., Isik, B., Ugraskan, V., and Cankurtaran, O. (2022). "Batch sorption studies of toxic methylene blue dye onto chitosan *Capsella bursa-pastoris* composite microbeads," *Biomass Conversion and Biorefinery* 1-17. DOI: 10.1007/s13399-022-03680-x

Thabede, P. M., and Shooto, N. D. (2022). "Application of black cumin (*Nigella sativa* L.) seeds for the removal of metal ions and methylene blue from aqueous solutions," *Cogent Engineering* 9(1), article 2013419. DOI: 10.1080/23311916.2021.2013419

Ugraskan, V., Isik, B., Yazici O., and Cakar, F. (2022). "Removal of Safranine T by a highly efficient adsorbent (*Cotinus coggygria* leaves): Isotherms, kinetics, thermodynamics, and surface properties," *Surfaces and Interfaces* 28, article 101615. DOI: 10.1016/j.surfin.2021.101615

Vigneshwaran, S., Sirajudheen, P., Karthikeyan, P., and Meenakshi, S. (2021). "Fabrication of sulfur-doped biochar derived from tapioca peel waste with superior adsorption performance for the removal of Malachite green and Rhodamine B dyes," *Surfaces and Interfaces*, 23, 100920. DOI: 10.1016/j.surfin.2020.100920

Xu, R. K., Xiao, S. C., Yuan, J. H., and Zhao, A. Z. (2011). "Adsorption of methyl violet from aqueous solutions by the biochars derived from crop residues," *Bioresource Technol.* 102(22), 10293-10298. DOI: 10.1016/j.biortech.2011.08.089

Yimer, E. M., Tuem, K. B., Karim, A., Ur-Rehman, N., and Anwar, F. (2019). "*Nigella sativa* L. (black cumin): A promising natural remedy for wide range of illnesses," *Evid. Based Complementary Altern. Med.*, 2019, Article ID: 1528635. DOI: 10.1155/2019/1528635

Zazycki, M. A., Godinho, M., Perondi, D., Foletto, E. L., Collazzo, G. C., and Dotto, G. L. (2018). "New biochar from pecan nutshells as an alternative adsorbent for removing reactive red 141 from aqueous solutions," *J. Clean. Prod.* 171, 57-65. DOI: 10.1016/j.jclepro.2017.10.007

Zent, İ. (2019). *Soğuk Preslenmiş Cörek Otu Posalarından Protein Hidrolizatlarının Uretilmesi ve Hidrolizatların Biyoaktif Ozelliklerinin Değerlendirilmesi*, Master's Thesis, *The Graduate School of Natural and Applied Sciences of İstanbul Sabahattin Zaim University*, 1-3.

Article submitted: February 17, 2023; Peer review completed: March 11, 2023; Revised version received: March 20, 2023; Accepted: March 21, 2023; Published: March 27, 2023.
DOI: 10.15376/biores.18.2.3414-3439